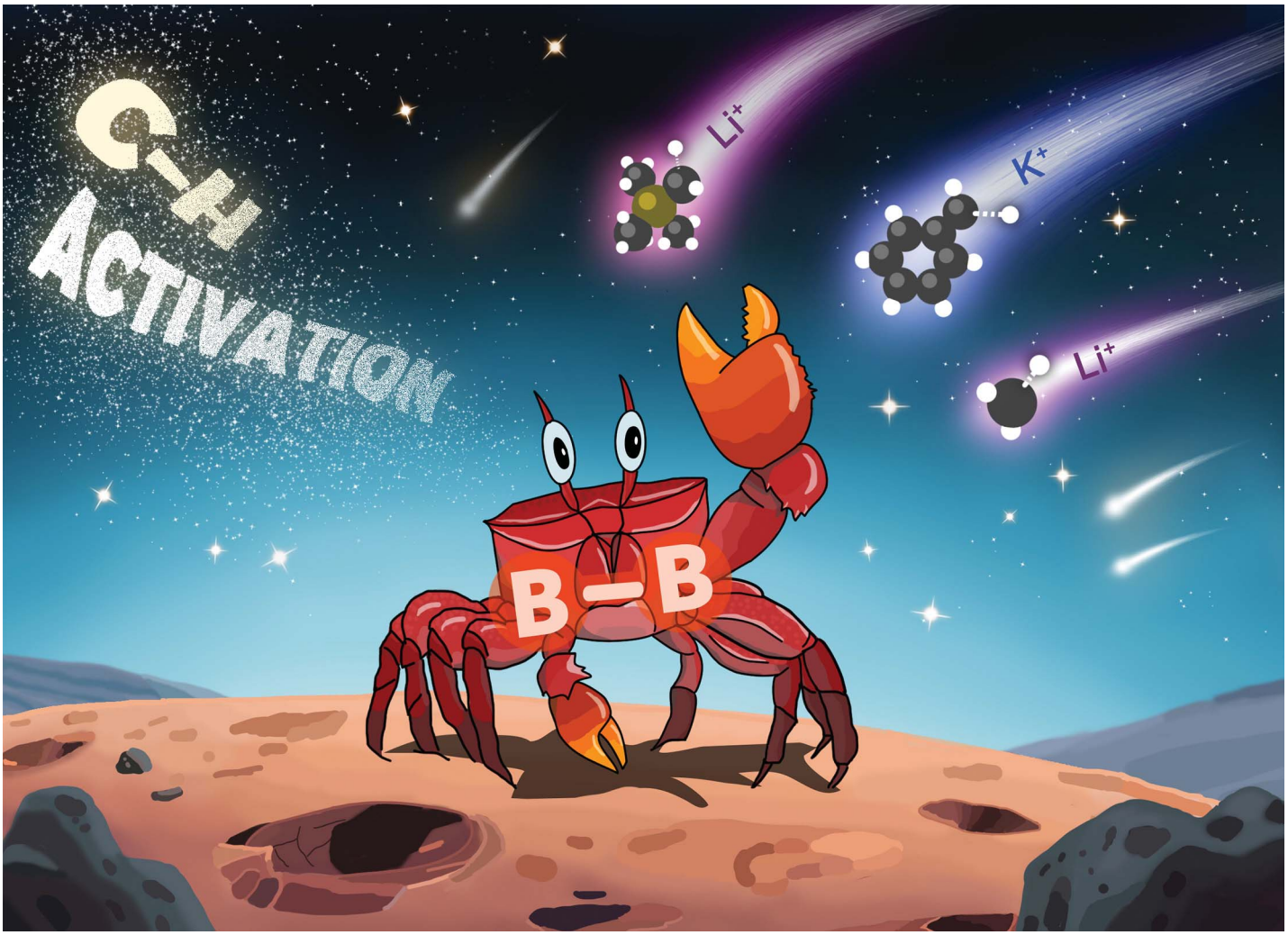

Showcasing research from Professor Xie's laboratory, Departments of Chemistry, Southern University of Science and Technology/The Chinese University of Hong Kong, China.

Regioselective C(sp^3)–H borylation *via* a diarylboryl anion surrogate in sp^2–sp^3 diboranes(5)

This paper reports a regioselective C(sp^3)–H borylation of sp^2–sp^3 diboranes(5) enabled by a highly reactive $[B(o\text{-tolyl})_2]^-$ surrogate. The surrogate preferentially inserts into α-C(sp^3)–H bonds of alkyl substituents, furnishing a series of 1,1-diborylalkyl compounds. When the substrate lacks α-C(sp^3)–H bonds, the process switches to β-C(sp^3)–H activation.

Image reproduced by permission of Xiaofeng Mao, Jie Zhang and Zuowei Xie from *Chem. Sci.,* 2025, **16**, 22314.

As featured in:

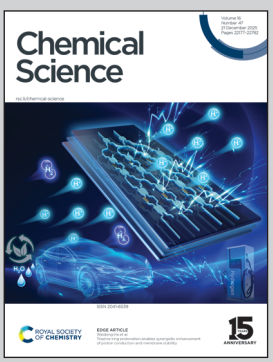

See Jie Zhang, Zuowei Xie *et al., Chem. Sci.,* 2025, **16**, 22314.

ROYAL SOCIETY OF CHEMISTRY

15 YEARS ANNIVERSARY

rsc.li/chemical-science

Registered charity number: 207890

Chemical Science

ROYAL SOCIETY OF CHEMISTRY

EDGE ARTICLE

View Article Online
View Journal | View Issue

Cite this: *Chem. Sci.*, 2025, **16**, 22314

All publication charges for this article have been paid for by the Royal Society of Chemistry

Received 17th September 2025
Accepted 4th November 2025

DOI: 10.1039/d5sc07180a

rsc.li/chemical-science

Regioselective C(sp^3)–H borylation *via* a diarylboryl anion surrogate in sp^2–sp^3 diboranes(5)

Xiaofeng Mao, [a] Jie Zhang *[a] and Zuowei Xie *[b]

Transition-metal-free C–H functionalization is a long-standing goal in synthetic chemistry. While a few main-group species have shown promise in C(sp^2)–H activation through insertion or nucleophilic aromatic substitution (S_NAr) pathways, C(sp^3)–H functionalization remains underdeveloped due to the intrinsic inertness of saturated carbon centers and the insufficient reactivity of reported main-group species. Herein, we report regioselective C(sp^3)–H borylation in sp^2–sp^3 diboranes(5), mediated by a highly reactive B(*o*-tolyl)$_2^-$ surrogate. It selectively inserts into α-C(sp^3)–H bonds of alkyl groups to generate a family of anionic 1,1-diborylalkyl species. The resulting anions are readily converted to neutral *gem*-diborylalkanes by using TMSOTf. In substrates lacking α-C(sp^3)–H bonds, β-C(sp^3)–H activation becomes operative, producing organic salts and olefins. Competitive experiments reveal a clear preference for α- over β-C(sp^3)–H activation. DFT calculations support a concerted insertion pathway and explain the preference for α- over β- and *ortho*-C–H activation. This study showcases the potential of reactive diarylboryl anion surrogates as powerful reagents for achieving regioselective C(sp^3)–H borylation and expands the synthetic landscape of main-group-element-mediated C–H activation.

Introduction

Carbene, featuring a divalent carbon center and a lone pair as well as an empty p orbital (Scheme 1a), has emerged as a significant building block in fundamental organic synthesis,[1–3] for example, C–H functionalization.[3] In comparison to the explosive development of carbene chemistry, the studies on anionic six-electron group 13 analogues are relatively rare.[4–17]

Typically, replacing the divalent carbon atom in carbenes with less electronegative group 13 elements enhances the reactivity of the resultant species,[15] which exhibit both nucleophilicity and tendency toward C(sp^2)–H oxidative addition. Accordingly, six- and eight-electron aluminyl anions (**I–II**, Scheme 1a) were unveiled by Yamashita[16,17] and Aldridge[18,19] independently to directly activate C(sp^2)–H bond of arenes *via* C(sp^2)–H oxidative addition or nucleophilic aromatic substitution (S_NAr). Notably, in the absence of internal π-donation from adjacent heteroatoms, two-carbon-substituted aluminyl anions (**II**) exhibit enhanced reactivity compared to their amino-substituted counterparts (**I**), enabling C(sp^2)–H activation under significantly milder conditions.[16] Analogously, diaminoboryl anions (**III**, Scheme 1a) were developed as borylation synthons to activate benzene[15] and benzylic C–H bonds.[10,14] Despite these advances, C(sp^3)–H functionalization by main-group species remains underdeveloped,[13] primarily due to the inherent inertness of saturated carbon atoms and the insufficient reactivity of reported main-group species. To overcome the strength of C(sp^3)–H bonds, access to main-group anions with substantially enhanced reactivity is essential.

Owing to the inert pair effect,[20,21] boryl anions generally exhibit higher reactivity than their aluminyl counterparts. Given their strong intrinsic reactivity and the desire to eliminate electronic stabilization from adjacent heteroatoms, it is highly desirable to leverage the most reactive group 13 anions—namely, two-carbon-substituted boryl anions (**IV**, Scheme 1a)—for the activation of C(sp^3)–H bonds. However, the pronounced ambiphilic boron center of **IV** severely compromises their stability, and as a result, such species can only be generated *in situ* and immediately undergo C–C or C–H bond activation.[10b]

Anionic sp^2–sp^3 diboranes(5), as emerging alternatives of boryl anions, have been utilized as nucleophilic sp^2 boryl anion transfer reagents, where the sp^2 boryl moiety is transferred for further nucleophilic transformations.[22] Generally, stable anionic sp^2–sp^3 diboranes(5) were prepared from the reactions of diborane(4) with alkoxides or fluoride ions.[23–29] In contrast, reactions of diborane(4) with carbanions result in either stable sp^2–sp^3 diboranes(5)[30–35] or intramolecular functionalization.[36–45]

In the context of intramolecular functionalization of carbanions (Scheme 1b), 1,2-metallate rearrangement of Bpin was achieved through treatment of B_2pin_2 with carbanions preinstalled with leaving groups (halogen, carbamate group, or

[a]*Department of Chemistry, The Chinese University of Hong Kong, Shatin, N. T., Hong Kong, China. E-mail: jiezhang@cuhk.edu.hk*

[b]*Shenzhen Grubbs Institute, Department of Chemistry, Southern University of Science and Technology, Shenzhen, Guangdong 518055, China. E-mail: zxie@cuhk.edu.hk*

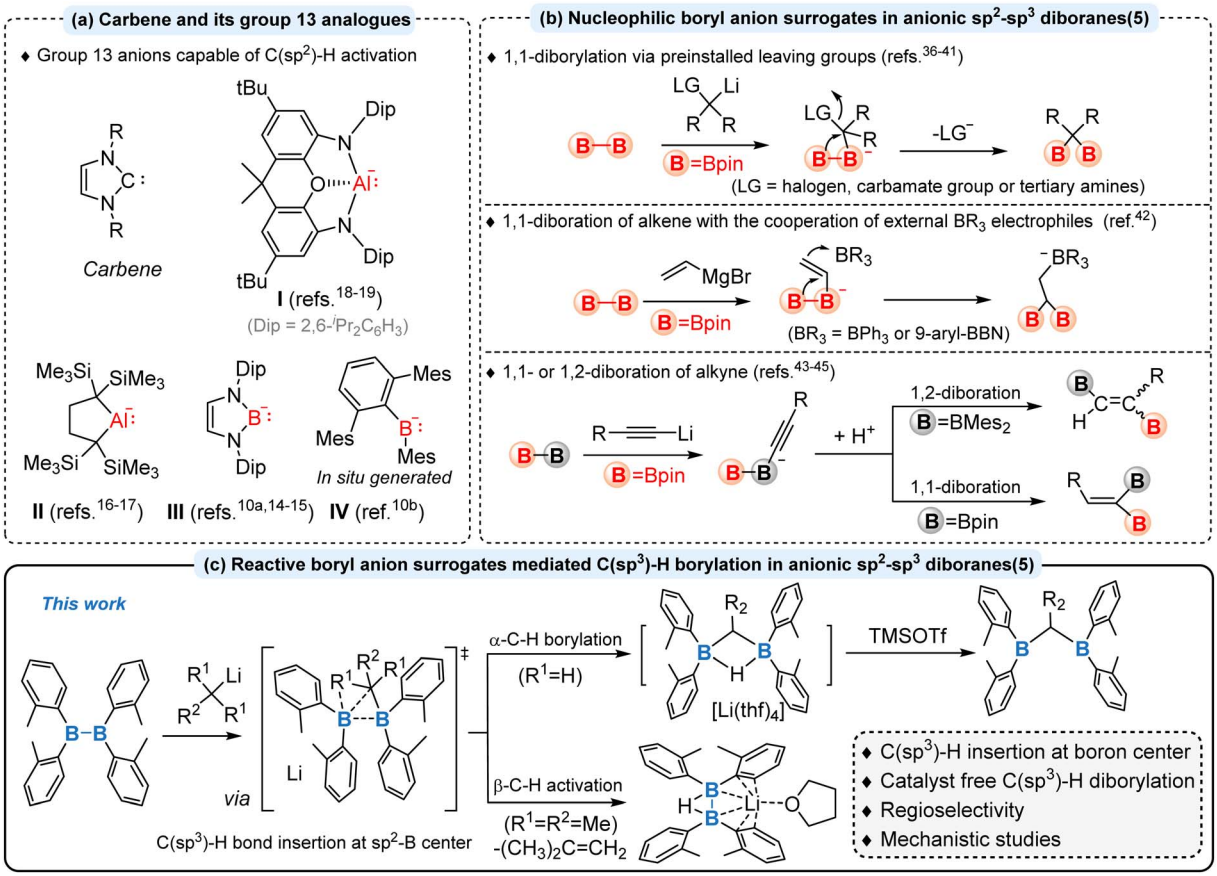

Scheme 1 Reactivity of group 13 anions and their surrogates in inter- and intra-molecular transformations. (a) Carbene and its group 13 analogues. (b) Nucleophilic boryl anion surrogates in anionic sp^2–sp^3 diboranes(5). (c) Reactive boryl anion surrogate-mediated C(sp^3)–H borylation in anionic sp^2–sp^3 diboranes(5).

tertiary amines), where 1,1-diborylated products were afforded *via* intramolecular nucleophilic attack of the Bpin moiety on pre-functionalized C atoms.[36–41] Subsequently, the intramolecular 1,1-diboration of the vinyl group without pre-functionalization was disclosed by Ingleson and co-workers through the treatment of B_2pin_2 with a vinyl Grignard reagent, which provided 1,1,2-triborylated alkanes in the incorporation of soft BR_3 electrophiles (*e.g.* BPh_3 or 9-aryl-BBN).[42] Alternatively, direct 1,1- or 1,2-diborations of alkynes were developed by Sawamura and Yamashita independently, in which reactions of different diboranes(4) with alkynyllithium led to either 1,1- or 1,2-diboration depending on the variation of substituents on the B atom in diboranes(4).[43–45] Previously, our group also unveiled that the B–B bond of transient {(aryl)B_2(*o*-tolyl)$_4$} anions can undergo nucleophilic aromatic substitution (S_NAr) with aryl rings, leading to C(sp^2)–H borylation of arenes.[46]

Previous studies on the intramolecular functionalization in sp^2–sp^3 diboranes(5) have primarily focused on nucleophilic reactions with electrophiles or unsaturated bonds (Scheme 1b), where the presence of an electrophilic site is essential for nucleophilic attack by sp^2 boryl anion surrogates. In contrast, their application in C(sp^3)–H activation remains challenging, mainly due to the lack of an electrophilic site and intrinsic inertness of C(sp^3)–H bonds toward nucleophiles.

Considering the enhanced reactivity of the two-carbon-substituted boryl anions (**IV**, Scheme 1a)[10b] compared to diaminoboryl anions (**III**), we sought to harness the highly reactive B(*o*-tolyl)$_2^-$ anion surrogate for intramolecular C(sp^3)–H borylation in sp^2–sp^3 diboranes(5). It has been reported that the reaction of diborane(4) dianionic salts with haloalkanes[13a] or treatment of doubly arylene-bridged diborane(6) with alkyllithium reagents[13b] resulted in the formation of sp^2–sp^3 diborane(5) alkyl species, which underwent intramolecular C(sp^3)–H activation of the alkyl group. Given the established α-C–H activation of borylated alkanes by Lewis bases (*e.g.* LiTMP, $LiNCy_2$, or MesLi),[47–52] we envisioned that treatment of B_2(*o*-tolyl)$_4$ with alkyllithium would generate a highly reactive B(*o*-tolyl)$_2^-$ anion surrogate capable of promoting intramolecular α-C(sp^3)–H activation, thereby affording 1,1-diborylalkyl lithium species.

Herein, we report the intramolecular C(sp^3)–H borylation in anionic [(alkyl)B_2(*o*-tolyl)$_4$] species induced by a highly reactive B(*o*-tolyl)$_2$ anion surrogate under mild conditions (Scheme 1c). Interestingly, when the carbanion lacks an α-C(sp^3)–H bond, the original pathway is shut down and β-C(sp^3)–H activation takes over, along with the formation of a (μ-hydrido)diborane(4) anion and an olefin. In addition, the bridging hydride of anionic 1,1-diborylated alkyl species can be removed upon

treatment with TMSOTf to generate neutral 1,1-diborylalkanes. In contrast to conventional transition metal-catalyzed C–H borylation methods,[53–56] this approach provides a catalyst-free method for regioselective C(sp^3)–H borylation and preparation of *gem*-diborylalkanes, which have recently emerged as important building blocks in organic synthesis and small molecule activation.[57–60]

Results and discussion

Intramolecular α-C(sp^3)–H borylation

We began our study by treatment of **1** with methyl lithium (1 : 1) in tetrahydrofuran (THF) solution at room temperature. Unlike reactions between heterocyclic diboranes and alkyl anions affording stable sp^2–sp^3 diboranes(5),[30,32–35] the utilization of non-heterocyclic diboranes resulted in a hydride-bridged diborylmethane anion [**2a**]Li in 95% yield (Scheme 2). The ^{11}B NMR spectrum of [**2a**]Li showed a broad singlet at −10.1 ppm, which was much high-field shifted compared to that of **1** (δ_B: 88.6 ppm),[61] but was comparable to the reported anionic diborylmethane species (δ_B: −14.0 ppm).[13b] The μ–H resonance was observed at 2.14 ppm in its ^{1}H{^{11}B} NMR spectrum. Single crystal X-ray analyses confirm the molecular structure of [**2a**]Li (Fig. 1). The distance between two boron atoms (1.982(5) Å) in [**2a**]Li lies in the range of non-covalent bonds which is comparable with the previously reported anionic diborylmethane (1.974(6) Å).[13b] Notably, no intramolecular *ortho*-C(sp^2)–H borylation[46] was observed. This preferential α-C(sp^3)–H borylation over *ortho*-C(sp^2)–H activation indicates that the B(*o*-tolyl)$_2^-$ anion surrogate functions primarily as a low-valent boron source engaged in α-C(sp^3)–H insertion rather than a nucleophile in the intramolecular transformation process.

To explore the compatibility of this methodology, **1** was treated with (trimethylsilyl)methyllithium or benzyl potassium (Scheme 2). Reaction of **1** with (trimethylsilyl)methyllithium afforded an anionic 1,1-diborylated alkane [**2b**]Li (δ_B: −8.7 ppm) in 91% yield, and the distance between two boron atoms

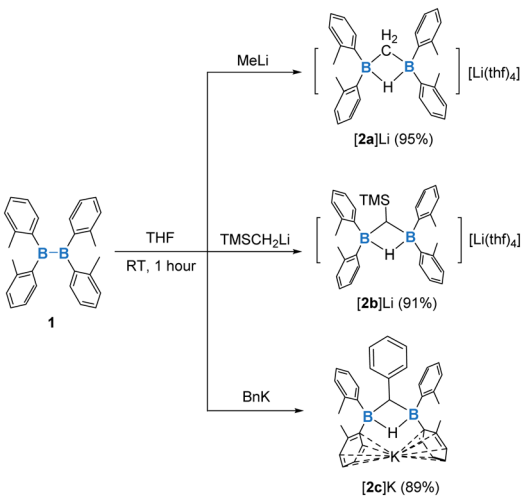

Scheme 2 Reaction of **1** with alkyllithium or benzylpotassium possessing α-C–H bonds.

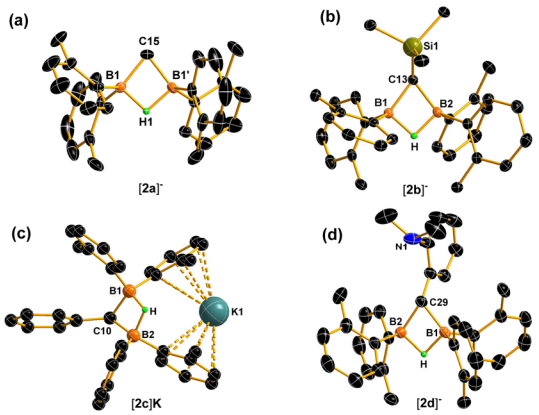

Fig. 1 Molecular structures of [**2a**]$^-$, [**2b**]$^-$, [**2c**]K and [**2d**]$^-$ (all hydrogen atoms and cations are omitted for clarity except for the bridging H atoms). Selected atom···atom distance (Å) and bond angles (deg.), (a) [**2a**]Li: B1···B1′ = 1.982(5); B1–C15–B1′ = 76.1(2). (b) [**2b**]Li: B1···B2 = 1.9578(18); B1–C13–B2 = 74.04(8). (c) [**2c**]K: B1···B2 = 1.971(2); B1–C10–B2 = 75.03(10). (d) [**2d**]Li: B1···B2 = 1.963(3); B1–C29–B2 = 73.94(12).

(1.958(2) Å) in [**2b**]Li (Fig. 1) is slightly shorter than that of [**2a**]Li (1.982(5) Å). In a similar manner, treatment of **1** with benzyl potassium generated [**2c**]K (δ_B: −7.7 ppm) in 89% yield with a B···B distance of 1.971(2) Å (Fig. 1). It should be noted that replacement of Li^+ by K^+ leads to an unsolvated species where two tolyl groups bind to the K^+. Unlike [**2a**]Li, two kinds of methyl signals (ratio 1 : 1) of tolyl groups were observed in the ^{1}H NMR spectra of both [**2b**]Li and [**2c**]K. This observation is likely attributed to magnetically inequivalent tolyl substituents, arising from reduced molecular symmetry. For steric reasons, no reaction was observed between **1** and TMS_2CHLi even under heating conditions.

In targeting a stable diborane anion prior to C(sp^3)–H borylation, we introduced a dimethylamino unit to the *ortho* position of a benzyl group with the expectation of blocking C–H activation and stabilizing the diborane(6) anion *via* the coordination of nitrogen to the boron atom. However, treatment of **1** with (*o*-$NMe_2C_6H_4$)CH_2Li at −78 °C resulted in the formation of 1,1-diborylated product [**2d**]Li (δ_B: −7.5 ppm) in 86% yield (Scheme 3). No expected diborane anionic salt was observed.

Intramolecular β-C(sp^3)–H activation

Regarding the above intramolecular α-C(sp^3)–H borylation, we attempted to examine the reaction with the carbanion without

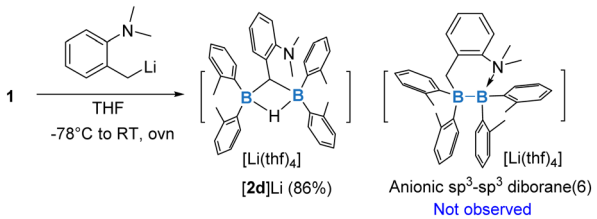

Scheme 3 Reaction of **1** with (*o*-$NMe_2C_6H_4$)CH_2Li.

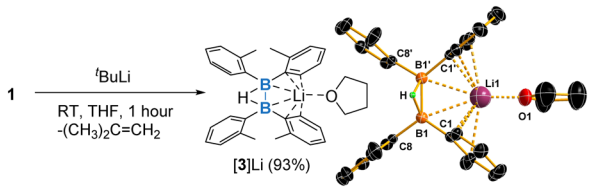

Fig. 2 Reaction of **1** with ^{t}BuLi and the molecular structure of [**3**]Li (all hydrogen atoms are omitted for clarity except for the bridging H atom). Selected bond distance (Å) and angles (deg.): B–B1′ = 1.642(6); C1–B1–B1′ = 123.98(14); C8–B1–B1′ = 120.97(14); C1–B1–C8 = 115.0(2).

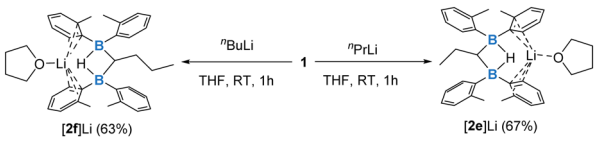

Scheme 4 Reactions of **1** with alkyllithium possessing both α- and β-C–H bonds.

α-C–H bonds (Fig. 2). Treatment of **1** with *tert*-butyllithium (1 : 1) in tetrahydrofuran afforded lithium (μ-hydrido)diborane(4) [**3**]Li in 93% yield accompanied by the formation of isobutylene (Fig. S37–S40). Single crystal X-ray analyses confirm the molecular structure of [**3**]Li as shown in Fig. 2. It features a B–B bond distance of 1.642(6) Å and shows a broad peak at 28.9 ppm in its ^{11}B NMR spectrum, which are comparable to previously reported sodium (μ-hydrido)diborane(4) (B–B bond length: 1.628(5) Å, δ_B: 30.2 ppm).[62]

Competing intramolecular α- and β-C(sp^3)–H borylation

Competition between intramolecular borylation at α-C(sp^3)–H and β-C(sp^3)–H positions was further explored experimentally through the reaction with ^{n}propyllithium or ^{n}butyllithium (Scheme 4). The reaction afforded either [**2e**]Li (δ_B: −11.6 ppm) or [**2f**]Li (δ_B: −10.2 ppm) as a major product in 67% or 63%, respectively. It was noteworthy that both α- and β-C–H activation proceeded even at a low temperature, but only a very small amount of β-C(sp^3)–H activation product [**3**]Li was observed as a minor product.

Single crystal X-ray diffraction revealed that the coordination between lithium cations and two tolyl groups exists (Fig. 3). As a result, two sets of methyl signals (1 : 1) of tolyl groups were observed in ^{1}H NMR spectra, which might be ascribed to the restricted rotation of the tolyl units.

Hydride abstraction reaction

The bridging hydride of anionic 1,1-diborylated alkyl species can be removed to generate neutral diborylated alkanes upon treatment with a hydride abstraction reagent.[46] For example, [**2a**]Li was treated with 3 equivalents of trimethylsilyl trifluoromethanesulfonate (TMSOTf) in acetonitrile to generate **4** as colorless oil in 90% yield (Scheme 5).[63]

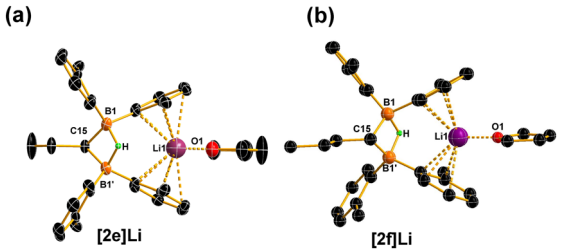

Fig. 3 Molecular structures of (a) [**2e**]Li and (b) [**2f**]Li (all hydrogen atoms are omitted for clarity except for the bridging H atoms). Selected atom···atom distance (Å) and angles (deg.) (a) [**2e**]Li: B(1)···B(1)′ = 1.982(7); B(1)–C(15)–B(1)′ = 76.1(3); (b) [**2f**]Li: B(1)···B(1)′ 1.956(4); B(1)–C(15)–B(1)′ 74.2(2).

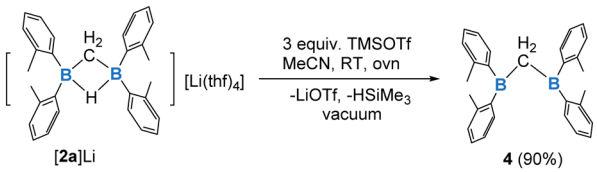

Scheme 5 Hydride abstraction of [**2a**]Li.

Mechanistic study

To locate the bridging hydride source in [**2a**]Li after the α-C(sp^3)–H borylation process, a deuterium labeling experiment was conducted and monitored by NMR spectroscopy. An equimolar reaction of deuterated methyllithium (CD_3Li) with **1** in THF afforded [**2a**]Li-d_3. Its ^{2}H NMR clearly showed the presence of the bridging deuterium at 2.12 ppm (Fig. 4), indicating that the bridging hydride in [**2a**]Li originated from methyllithium (Fig. S41–S46). This observation is reminiscent of the similar deuterium-labeling results from the reaction of doubly arylene-bridged diborane(6) with alkyllithium reagents.[13b]

Density functional theory (DFT) calculations at the B3LYP-D3/6-311g(d,p) level of theory were conducted to elucidate the possible reaction pathways and selectivity. To understand the superior selectivity of α-C(sp^3)–H borylation over β-C(sp^3)–H

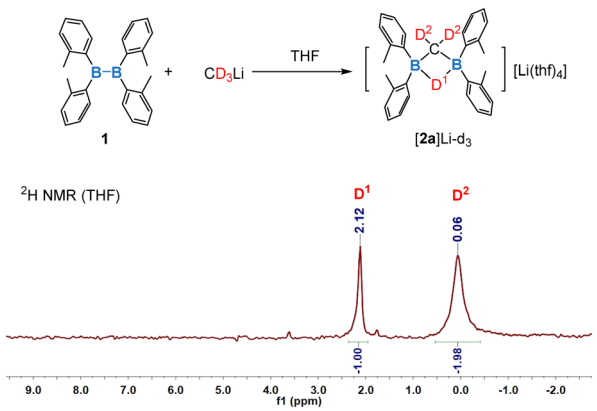

Fig. 4 Reaction and the ^{2}H NMR spectrum of **1** with CD_3Li in tetrahydrofuran.

and *ortho*-C(sp^2)–H borylation,[46] the reaction of ^{n}BuLi with **1** was chosen as the model for computational study. Two proposed pathways, concerted insertion and stepwise deprotonation pathways, were proposed for both α- and β-C(sp^3)–H borylation (Fig. S47 and S48). Comparing the energy barriers (*vide infra*) of rate-determining steps in all proposed pathways, the concerted insertion pathway in α-C(sp^3)–H borylation (15.0 kcal mol^{-1}) is energetically more favorable than the stepwise deprotonation pathway (38.2 kcal mol^{-1}) (Fig. S47), as well as both pathways in β-C(sp^3)–H borylation (stepwise deprotonation pathway: 38.2 kcal mol^{-1}, concerted insertion pathway: 54.4 kcal mol^{-1}) (Fig. S48). In line with our previously reported C(sp^2)–H borylation,[46] three pathways were proposed for *ortho*-C(sp^2)–H borylation, including nucleophilic substitution (27.9 kcal mol^{-1}), deprotonation (38.2 kcal mol^{-1}) and insertion (44.8 kcal mol^{-1}) (Fig. S49). Energetically, the concerted insertion pathway in α-C(sp^3)–H borylation represented the most rational reaction route, which might contribute to the excellent regioselectivity and chemoselectivity of such transformation.

For simplicity, only the energetically most favorable pathways for α-C(sp^3)–H borylation (black), β-C(sp^3)–H borylation (red), and *ortho*-C(sp^2)–H borylation (blue) are exhibited in Fig. 5 as the representatives. All these proposed mechanisms start from the intermediate **A_1**, which is generated from the addition of ^{n}BuLi to one B atom in B_2(*o*-tolyl)$_4$. The concerted insertion mechanism for α-C(sp^3)–H borylation (black) continues from the synchronous B–B bond cleavage and α-C(sp^3)–H insertion into the boron center to give **A_2** *via* **A_TS1** with an energy barrier of 15.0 kcal mol^{-1}. This pathway is reminiscent of the previously reported intramolecular C–H insertion by the carbene-like [BFlu]$^-$ anion surrogate.[13b] In addition, the natural bond orbital (NBO) analyses indicate that both B–B and α-C–H bonds in **A_TS1** are highly polarized, consistent with the role of such anionic sp^2–sp^3 diboranes(5) as diarylboryl anion surrogates in the reaction (see Fig. S51 in the SI). **A_2** goes through further hydride migration to form a bridging hydride species **[2f]Li′**. The stepwise deprotonation mechanism for β-C(sp^3)–H borylation (red) is disclosed as a multi-step reaction. The B–B bond cleavage in **A_1** occurs to afford boryllithium complex **B_1** *via* **A_TS2**, and then the boryl anion in **B_1** attacks the β-C(sp^3)–H proton of the alkyl group to generate **B_2** *via* **B_TS1**. Subsequently, **B_2** undergoes further hydride migration to form a bridging hydride species **B_3**. In this route, the B–B bond cleavage process (**A_1** → **B_1**) represents the rate-determining step with an energy barrier of 38.2 kcal mol^{-1}. Similarly, *ortho*-C(sp^2)–H borylation (blue) prefers a nucleophilic aromatic substitution (S_NAr) mechanism, which is consistent with the previously reported one.[46] In **A_1**, the cleavage of B–B bonds and subsequent nucleophilic addition of B to *ortho*-C of the *o*-tolyl group gives **C_4** *via* **C_TS2**. And then, the hydride of **C_4** migrates from the C to B atom *via* **C_TS3** to generate **C_2**, which undergoes further transformation to afford the final product **C_3**. This route possesses the rate-determining step (**A_1** → **C_4**) with an energy barrier of 27.9 kcal mol^{-1}. Of note, the energy barrier of 27.9 kcal mol^{-1} in *ortho*-C(sp^2)–H borylation is significantly larger than both 15.0 kcal mol^{-1} of

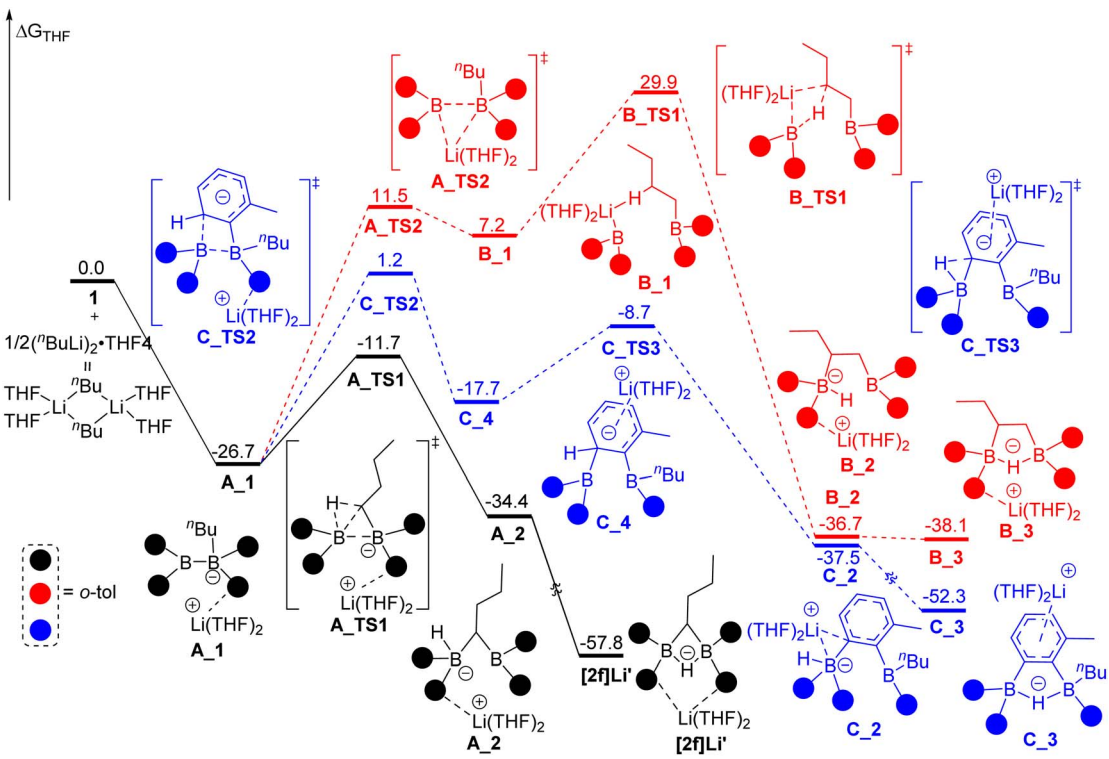

Fig. 5 Energy profiles of the DFT-based mechanism for α-C(sp^3)–H borylation (black), β-C(sp^3)–H borylation (red), and *ortho*-C(sp^2)–H borylation (blue), including schematic structures of transition states, calculated at the B3LYP-D3/6-311g(d,p) level of theory. Relative Gibbs free energies are given in kcal mol^{-1}.

concerted α-C(sp^3)–H insertion and 10.6 kcal mol^{-1} of previously reported *ortho*-C(sp^2)–H borylation,[46] which may be attributed to steric and electronic effects from the methyl substituent on the *o*-tolyl group.[17] The above computational studies unveil that α-C(sp^3)–H borylation is energetically more favorable than both β-C(sp^3)–H activation and *ortho*-C(sp^2)–H borylation, which is in line with the experimental results.

In addition, the mechanism for reaction of **1** with ^{t}BuLi was also investigated by DFT study (Fig. 6). Two plausible reaction pathways, stepwise (black) and concerted (blue) mechanisms, are proposed for β-C(sp^3)–H activation of ^{t}BuLi, and both initiate from the intermediate **D_1**, which is generated from the nucleophilic addition of ^{t}BuLi to one B atom in B_2(*o*-tolyl)$_4$. The concerted mechanism (blue) proceeds from the synchronous β-C(sp^3)–H deprotonation in the ^{t}Bu group and elimination of isobutene to give **D_2** *via* **D_TS1** with an energy barrier of 28.9 kcal mol^{-1}, followed by further hydride migration to generate **[3]Li′**. On the other hand, the stepwise mechanism (black) involves a multi-step reaction. The cleavage of B–B bonds in **D_1** occurs to afford boryllithium complex **D_3** *via* **D_TS2**, and then the boryl anion in **D_3** attacks the β-C(sp^3)–H proton of the ^{t}Bu group to generate **D_4** *via* **D_TS3**, where **D_4** consists of a di(*o*-tolyl)hydroborane unit and a three-membered cyclic borate lithium species. Subsequently, the formation of B–B bonds and elimination of isobutene occur to give **D_2** *via* **D_TS4**,[64,65] accompanied by further hydride migration to generate **[3]Li′**. In this route, the process (**D_4** → **D_2**) represents the rate-determining step with an energy barrier of 25.9 kcal mol^{-1}. The above computational studies reveal that the stepwise deprotonation mechanism is energetically more favorable than concerted mechanisms, consistent with previously reported deprotonation processes mediated by boryl anions.[14,15] Such an energy barrier for stepwise β-C(sp^3)–H activation is significantly larger than that of 15.0 kcal mol^{-1} for α-C(sp^3)–H borylation, as shown in Fig. 5, which is in line with the superior selectivity of intramolecular α-C(sp^3)–H borylation over β-C(sp^3)–H activation in competitive experiments.

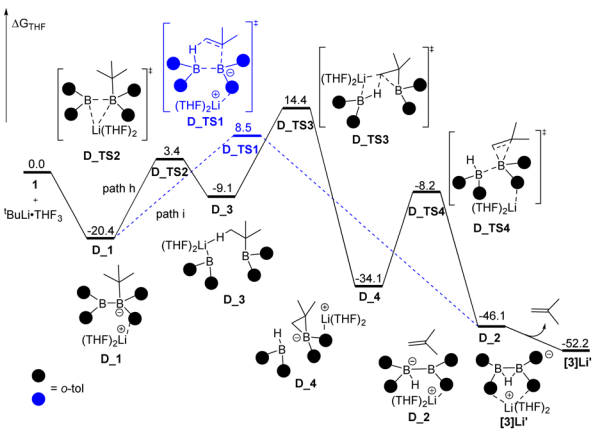

Fig. 6 Energy profiles of the DFT-based mechanism for β-C(sp^3)–H activation of ^{t}BuLi, including schematic structures of transition states, calculated at the B3LYP-D3/6-311g(d,p) level of theory. Relative Gibbs free energies are given in kcal mol^{-1}.

Conclusions

In summary, we have described transition-metal-free C(sp^3)–H borylation in sp^2–sp^3 diboranes(5) mediated by the highly reactive B(*o*-tolyl)$_2$ anion surrogate. The extremely reactive B(*o*-tolyl)$_2$ anion surrogate, among the most reactive group 13 species, exhibits sufficient reactivity and selectively promotes α-C(sp^3)–H borylation over β-C(sp^3)–H and *ortho*-C(sp^2)–H positions, affording 1,1-diborylalkyl anions *via* a concerted insertion pathway, as supported by computational studies. In the absence of α-C(sp^3)–H bonds, the reaction diverges to β-C(sp^3)–H activation, leading to lithium (μ-hydrido)diborane(4) and olefin products—also energetically feasible according to computational analysis. Moreover, the resulting anionic 1,1-diborylalkyl species can be readily converted to neutral *gem*-diborylalkanes upon treatment with TMSOTf. This work establishes a new strategy for main-group-mediated C(sp^3)–H activation and highlights the synthetic potential of sp^2–sp^3 diboranes(5) in organoboron chemistry. The use of reactive boryl anion surrogates offers a new insight into main-group-mediated site-selective C–H functionalization and catalyst-free activation of inert bonds.

Author contributions

Z. X. generated and managed the project. X. M. carried out the experiments and characterization of the reaction products as well as prepared the supporting information. J. Z. carried out the DFT calculations. All authors prepared the manuscript.

Conflicts of interest

The authors declare no competing financial interest.

Data availability

CCDC 2476189–2476195 for [**2a**]Li, [**2b**]Li, [**2c**]K, [**2d**]Li, [**2e**]Li, [**2f**]Li and [**3**]Li contain the supplementary crystallographic data for this paper.[66a–g]

The data that support the findings of this study are available within the main text and its supplementary information (SI). Supplementary information is available. See DOI: **https://doi.org/10.1039/d5sc07180a**.

Acknowledgements

We gratefully acknowledge the financial support from the National Natural Science Foundation of China (Project No. 22331005 to Z. X. and 22201238 to J. Z.) and the Shenzhen Science and Technology Program (Project No. KQTD20221101093558015).

Notes and references

1 P. Bellotti, M. Koy, M. N. Hopkinson and F. Glorius, *Nat. Rev. Chem.*, 2021, **5**, 711–725.

2 S. K. Kushvaha, A. Mishra, H. W. Roesky and K. C. Mondal, *Chem.–Asian J.*, 2022, **17**, e2021013.
3 Y. He, Z. Huang, K. Wu, J. Ma, Y. G. Zhou and Z. Yu, *Chem. Soc. Rev.*, 2022, **51**, 2759–2852.
4 Y. Segawa, Y. Suzuki, M. Yamashita and K. Nozaki, *J. Am. Chem. Soc.*, 2008, **130**, 16069–16079.
5 R. J. Schwamm, M. D. Anker, M. Lein and M. P. Coles, *Angew. Chem., Int. Ed.*, 2019, **58**, 1489–1493.
6 E. S. Schmidt, A. Jockisch and H. Schmidbaur, *J. Am. Chem. Soc.*, 1999, **121**, 9758–9759.
7 R. J. Baker, R. D. Farley, C. Jones, M. Kloth and D. M. Murphy, *J. Chem. Soc., Dalton Trans.*, 2002, **2002**, 3844–3850.
8 R. J. Schwamm, M. D. Anker, M. Lein, M. P. Coles and C. M. Fitchett, *Angew. Chem., Int. Ed.*, 2018, **57**, 5885–5887.
9 C. Cui, H. W. Roesky, H.-G. Schmidt, M. Noltemeyer, H. Hao and F. Cimpoesu, *Angew. Chem., Int. Ed.*, 2000, **39**, 4274–4276.
10 (*a*) A. V. Protchenko, P. Vasko, M. Á. Fuentes, J. Hicks, D. Vidovic and S. Aldridge, *Angew. Chem., Int. Ed.*, 2021, **60**, 2064–2068; (*b*) C. Zhang, J. Wang, X. Zhang, P. Dabringhaus, W. Shi, K. Qian, C.-L. Deng, C. C. Cummins and R. J. Gilliard Jr, *J. Am. Chem. Soc.*, 2025, **147**, 22033–22040.
11 W. Lu, H. Hu, Y. Li, R. Ganguly and R. Kinjo, *J. Am. Chem. Soc.*, 2016, **138**, 6650–6661.
12 (*a*) J. Hicks, P. Vasko, J. M. Goicoechea and S. Aldridge, *Angew. Chem., Int. Ed.*, 2021, **60**, 1702–1713; (*b*) Y. Segawa, M. Yamashita and K. Nozaki, *Science*, 2006, **314**, 113–115.
13 (*a*) H. Budy, T. Kaese, M. Bolte, H. W. Lerner and M. Wagner, *Angew. Chem., Int. Ed.*, 2021, **60**, 19397–19405; (*b*) T. Kaese, T. Trageser, H. Budy, M. Bolte, H.-W. Lerner and M. Wagner, *Chem. Sci.*, 2018, **9**, 3881–3891.
14 N. Dettenrieder, Y. Aramaki, B. M. Wolf, C. Maichle-Mössmer, X. Zhao, M. Yamashita, K. Nozaki and R. Anwander, *Angew. Chem., Int. Ed.*, 2014, **53**, 6259–6262.
15 T. Ohsato, Y. Okuno, S. Ishida, T. Iwamoto, K.-H. Lee, Z. Lin, M. Yamashita and K. Nozaki, *Angew. Chem., Int. Ed.*, 2016, **55**, 11426–11430.
16 S. Kurumada, S. Takamori and M. Yamashita, *Nat. Chem.*, 2020, **12**, 36–39.
17 S. Kurumada, K. Sugita, R. Nakano and M. Yamashita, *Angew. Chem., Int. Ed.*, 2020, **59**, 20381–20384.
18 J. Hicks, P. Vasko, J. M. Goicoechea and S. Aldridge, *Nature*, 2018, **557**, 92–95.
19 J. Hicks, P. Vasko, J. M. Goicoechea and S. Aldridge, *J. Am. Chem. Soc.*, 2019, **141**, 11000–11003.
20 M. He, C. Hu, R. Wei, X.-F. Wang and L. L. Liu, *Chem. Soc. Rev.*, 2024, **53**, 3896–3951.
21 C.-H. Chen, M.-L. Tsai and M.-D. Su, *Organometallics*, 2006, **25**, 2766–2773.
22 R. D. Dewhurst, E. C. Neeve, H. Braunschweig and T. B. Marder, *Chem. Commun.*, 2015, **51**, 9594–9607.
23 A. Bonet, C. Pubill-Ulldemolins, C. Bo, H. Gulyás and E. Fernández, *Angew. Chem., Int. Ed.*, 2011, **50**, 7158–7161.
24 C. Borner and C. Kleeberg, *Eur. J. Inorg. Chem.*, 2014, **2014**, 2486–2489.
25 S. Pietsch, E. C. Neeve, D. C. Apperley, R. Bertermann, F. Mo, D. Qiu, M. S. Cheung, L. Dang, J. Wang, U. Radius, Z. Lin, C. Kleeberg and T. B. Marder, *Chem.–Eur. J.*, 2015, **21**, 7082–7098.
26 C. Kleeberg, L. Dang, Z. Lin and T. B. Marder, *Angew. Chem., Int. Ed.*, 2009, **48**, 5350–5354.
27 A. Bonet, H. Gulyás and E. Fernández, *Angew. Chem., Int. Ed.*, 2010, **49**, 5130–5134.
28 T. P. Blaisdell, T. C. Caya, L. Zhang, A. Sanz-Marco and J. P. Morken, *J. Am. Chem. Soc.*, 2014, **136**, 9264–9267.
29 Y. Nagashima, K. Hirano, R. Takita and M. Uchiyama, *J. Am. Chem. Soc.*, 2014, **136**, 8532–8535.
30 R. B. Bedford, P. B. Brener, E. Carter, T. Gallagher, D. M. Murphy and D. R. Pye, *Organometallics*, 2014, **33**, 5940–5943.
31 J. Zheng, Y. Wang, Z. Li and H. Wang, *Chem. Commun.*, 2015, **51**, 5505–5508.
32 A.-F. Pécharman, A. L. Colebatch, M. S. Hill, C. L. McMullin, M. F. Mahon and C. Weetman, *Nat. Commun.*, 2017, **8**, 15022.
33 A.-F. Pécharman, M. S. Hill, C. L. McMullin and M. F. Mahon, *Angew. Chem., Int. Ed.*, 2017, **56**, 16363–16366.
34 A.-F. Pécharman, M. S. Hill and M. F. Mahon, *Dalton Trans.*, 2018, **47**, 7300–7305.
35 A.-F. Pécharman, M. S. Hill and M. F. Mahon, *Angew. Chem., Int. Ed.*, 2018, **57**, 10688–10691.
36 T. Hata, H. Kitagawa, H. Masai, T. Kurahashi, M. Shimizu and T. Hiyama, *Angew. Chem., Int. Ed.*, 2001, **40**, 790–792.
37 M. Shimizu, M. Schelper, I. Nagao, K. Shimono, T. Kurahashi and T. Hiyama, *Chem. Lett.*, 2006, **35**, 1222–1223.
38 H. Zhao, M. Tong, H. Wang and S. Xu, *Org. Biomol. Chem.*, 2017, **15**, 3418–3422.
39 T. Fang, L. Xu, Y. Qin, N. Jiang and C. Liu, *Chin. J. Inorg. Chem.*, 2023, **43**, 777–780.
40 Y. Qin, L. Xu, J. Xu and C. Liu, *Chin. J. Inorg. Chem.*, 2023, **43**, 1868–1874.
41 T. Fang, L. Wang, M. Wu, X. Qi and C. Liu, *Angew. Chem., Int. Ed.*, 2024, **63**, e202315227.
42 V. Fasano, J. Cid, R. J. Procter, E. Ross and M. J. Ingleson, *Angew. Chem., Int. Ed.*, 2018, **57**, 13293–13297.
43 C. Kojima, K.-H. Lee, Z. Lin and M. Yamashita, *J. Am. Chem. Soc.*, 2016, **138**, 6662–6669.
44 A. Morinaga, K. Nagao, H. Ohmiya and M. Sawamura, *Angew. Chem., Int. Ed.*, 2015, **54**, 15859–15862.
45 L. Wu, C. Kojima, K.-H. Lee, S. Morisako, Z. Lin and M. Yamashita, *Chem. Sci.*, 2021, **12**, 9806–9815.
46 X. Mao, Z. Lu, J. Zhang and Z. Xie, *Angew. Chem., Int. Ed.*, 2024, **63**, e202317614.
47 M. W. Rathke and R. Kow, *J. Am. Chem. Soc.*, 1972, **94**, 6854–6856.
48 R. Kow and M. Rathke, *J. Am. Chem. Soc.*, 1973, **95**, 2715–2716.
49 A. Pelter, B. Singaram, L. Warren and J. W. Wilson, *Tetrahedron*, 1993, **49**, 2965–2978.
50 A. Pelter, B. Singaram, L. Williams and J. W. Wilson, *Tetrahedron Lett.*, 1983, **24**, 623–626.

51 A. Pelter, L. Williams and J. W. Wilson, *Tetrahedron Lett.*, 1983, **24**, 627–630.
52 A. Pelter, B. Singaram and J. W. Wilson, *Tetrahedron Lett.*, 1983, **24**, 631–634.
53 (*a*) Y.-M. Tian, X.-N. Guo, H. Braunschweig, U. Radius and T. B. Marder, *Chem. Rev.*, 2021, **121**, 3561–3597; (*b*) I. A. I. Mkhalid, J. H. Barnard, T. B. Marder, J. M. Murphy and J. F. Hartwig, *Chem. Rev.*, 2010, **110**, 890–931; (*c*) J. F. Hartwig, *Chem. Soc. Rev.*, 2011, **40**, 1992–2002; (*d*) A. Ros, R. Fernández and J. M. Lassaletta, *Chem. Soc. Rev.*, 2014, **43**, 3229–3243; (*e*) Y.-M. Tian, X.-N. Guo, H. Braunschweig, U. Radius and T. B. Marder, *Chem. Rev.*, 2021, **121**, 3561–3597.
54 J. Hu, J. Lv and Z. Shi, *Trends Chem.*, 2022, **4**, 685–698.
55 R. Oeschger, B. Su, I. Yu, C. Ehinger, E. Romero, S. He and J. Hartwig, *Science*, 2020, **368**, 736–741.
56 J.-L. Han, Y. Qin, C.-W. Ju and D. Zhao, *Angew. Chem., Int. Ed.*, 2020, **59**, 6555–6560.
57 A. B. Cuenca and E. Fernández, *Chem. Soc. Rev.*, 2021, **50**, 72–86.
58 R. J. Maza, J. J. Carbó and E. Fernández, *Adv. Synth. Catal.*, 2021, **363**, 2274–2289.
59 R. Nallagonda, K. Padala and A. Masarwa, *Org. Biomol. Chem.*, 2018, **16**, 1050–1064.
60 A. Yeganeh-Salman, J. Yeung, L. Miao and D. W. Stephan, *Dalton Trans.*, 2024, **53**, 1178–1189.
61 N. Tsukahara, H. Asakawa, K.-H. Lee, Z. Lin and M. Yamashita, *J. Am. Chem. Soc.*, 2017, **139**, 2593–2596.
62 X. Mao, J. Zhang, Z. Lu and Z. Xie, *Chem. Sci.*, 2022, **13**, 3009–3013.
63 S. Akiyama, K. Yamada and M. Yamashita, *Angew. Chem., Int. Ed.*, 2019, **58**, 11806–11810.
64 C. R. P. Millet, D. R. Willcox, G. S. Nichol, C. S. Anstöter and M. J. Ingleson, *Angew. Chem., Int. Ed.*, 2024, **64**, e202419094.
65 C. Yan and R. Kinjo, *Angew. Chem., Int. Ed.*, 2022, **61**, e202211800.
66 (*a*) CCDC 2476189: Experimental Crystal Structure Determination, 2025, DOI: **10.5517/ccdc.csd.cc2p3p2l**; (*b*) CCDC 2476190: Experimental Crystal Structure Determination, 2025, DOI: **10.5517/ccdc.csd.cc2p3p3m**; (*c*) CCDC 2476191: Experimental Crystal Structure Determination, 2025, DOI: **10.5517/ccdc.csd.cc2p3p4n**; (*d*) CCDC 2476192: Experimental Crystal Structure Determination, 2025, DOI: **10.5517/ccdc.csd.cc2p3p5p**; (*e*) CCDC 2476193: Experimental Crystal Structure Determination, 2025, DOI: **10.5517/ccdc.csd.cc2p3p6q**; (*f*) CCDC 2476194: Experimental Crystal Structure Determination, 2025, DOI: **10.5517/ccdc.csd.cc2p3p7r**; (*g*) CCDC 2476195: Experimental Crystal Structure Determination, 2025, DOI: **10.5517/ccdc.csd.cc2p3p8s**.